An Investigation of the Morphology of Amorphous/Semicrystalline Nylon Blends Using Small-Angle X-ray Scattering

Mark E. Myers* and Andrew M. Wims

Analytical Chemistry Department, General Motors Research Laboratories, Warren, Michigan 48090-9050

Thomas S. Ellis

Polymers Department, General Motors Research Laboratories, Warren, Michigan 48090-9050

John Barnes

National Institute of Standards and Technology, Gaithersburg, Maryland 20899

Received September 5, 1989; Revised Manuscript Received November 27, 1989

ABSTRACT: Blends of nylon 6 and nylon 66, respectively, containing a miscible noncrystallizable polyamide have been investigated by using small-angle X-ray scattering, SAXS. The relative constancy of both the local linear crystallinity and the interlamellar spacing, or long period, as the concentration of the noncrystallizable component increased to 75% by weight, has been interpreted as the result of rejection of the latter from the interlamellar regions. For some blend compositions and under certain crystallization conditions, this interpretation is open to question; however, the presence of a heterogeneous mixed noncrystalline morphology is also supported by calorimetric studies, which indicate unusual glass transition, T_g, behavior. Measurements of the diffuse boundary thickness show a dependence on blend composition which indicates that this region consists of nylon 6 or nylon 66. There is no substantive difference in the behavior of blends containing either nylon 6 or nylon 66, as the crystallizable component, with the noncrystallizable polyamide.

Introduction

The development of structure in a crystallizable polymer during solidification from the melt is influenced by many intrinsic and external variables. An additional level of complexity may be imparted by the introduction of a noncrystallizable polymer diluent. Consequently, there are a number of different kinetic and thermodynamic situations that will determine how this diluent is distributed throughout the mixed amorphous–crystalline matrix. Morphological studies[1,2] involving polymer mixtures in which components differed only in tacticity have highlighted the role of a segregation of noncrystallizable species on the observed spherulitic texture. Similar studies[3] on polymer–polymer blends consisting of chemically dissimilar and possibly interacting, components have also shown striking adjustments to the spherulitic texture developed during crystallization. While many of the issues germane to these processes have already been addressed,[4] recent experiments[5] have shown that the addition of small amounts (~1%) of polymeric diluents can produce substantial morphological changes and a depletion of nucleating sites in a crystallizable polymer. Evidently there is still much which is not understood concerning structure development in miscible crystallizable polymer mixtures.

The miscibility of the noncrystallizable polyamide nylon 3Me6T (the chemical structure is shown in Table I) in aliphatic polyamides is well-documented in the literature.[6-8] In particular, nylon 6 forms miscible blends across the entire range of composition but retains the ability to crystallize, leading to a volume-filling spherulitic morphology, even up to a high nylon 3Me6T content.[6] Calorimetric and simple optical microscopic examination of crystallized blends have also shown that the nylon 6 component is capable of crystallizing to an extent equivalent to that measured in the pure state and is accompanied by noticeable changes of spherulitic appearance. The changes, however, were not as dramatic, for example, as those noted by Briber and Khoury[3] on a different but equivalent blend system. In addition to these observations it has been noted that crystallized blends exhibit unusual glass transition (T_g) behavior characteristic of a heterogeneous mixed amorphous phase. Mainly restricted to the middle of the composition range, a distinct broadening, and in some instances a discernible bimodal character, can be seen in the change of heat capacity (ΔC_p) associated with T_g. This observation contrasts markedly with that for the completely amorphous blends, produced by quench cooling from the melt, which display singular and relatively abrupt transitional behavior. Several other reports of miscible crystalline/amorphous blends possessing unusual features related to heterogeneities of the mixed amorphous regions have been described in the literature.[9,10] We believe that such heterogeneities are not the result of immiscibility of the components and

Table I
Structure and Properties of the Polymers

	nylon 6 [$(CH_2)_5NHCO$]	nylon 66 [$NH(CH_2)_6NH$-$CO(CH_2)_4CO$]	nylon 3Me6T [$COPhCONHCH_2C$-$(Me)_2CH_2CHMe(CH_2)_2NH$]
T_g, °C	40	45	147
T_m, °C	223	262	
$10^{-3}M_n$	41	31	20
$10^{-3}M_w$	120	92.5	63
ρ_a, g cm^{-3}	(1.08)[a]	(1.07)[a]	1.12
ρ_c, g cm^{-3}	(1.24)[b]	(1.24)[b]	

[a] Wunderlich, B. *Macromolecular Physics*; Academic Press: New York and London, 1973; Vol. 1, p 389. [b] Wunderlich, B. *Ibid.*, pp 132–3.

0024-9297/90/2223-2807$02.50/0

are not related to any large-scale thermodynamic phase separation phenomenon but rather that they are morphological in origin, imposed during the crystallization process.

The nondestructive technique of small-angle X-ray scattering (SAXS) has evolved to provide unique information on the morphology of crystallized polymer mixtures.[11-17] The application of this technique has been shown to provide the usual crystallographic information as well as detailed information on the nature of the crystalline/amorphous interface. In this paper we have followed closely the SAXS data reduction and analysis procedures used by other workers in their studies of semicrystalline polymers which have a lamellar structure and which have been blended with noncrystallizable polymers. It was our expectation that SAXS would put additional light on the morphological behavior of the blends of two crystallizable polyamides, nylon 6 and nylon 66, with the noncrystallizable polyamide nylon 3Me6T.

Experimental Section

Materials and Preparation. A complete description of the materials used in this study is available in the literature;[6,7] however, the essential details are also listed in Table I. Nylon 3Me6T is a condensation product of predominantly 2,2,4-trimethyl-1,6-hexanediamine and benzene-1,4-dicarboxylic acid and was obtained as Trogamid T from the Dynamit Nobel Co. The chemical structure is shown in Table I. Nylon 6 (Zytel 211) and nylon 66 (Zytel 101) were obtained from Du Pont, and blends containing 0, 25, 50, and 75% by weight of nylon 3Me6T were obtained by coprecipitation from a common solvent in the manner described previously.[6,7] Thin disks (12 mm × 0.5 mm) of each sample were prepared by compression molding using a heated hydraulic press. The molten samples were immediately transferred to a separate press maintained at 155 or 200 °C, as required, where they were annealed for 16 h.

Thermal Analysis. All samples were characterized by DSC immediately after annealing by using a Perkin-Elmer Series 7 calorimeter, programmed at a heating rate of 10 °C/min. Temperature and energy calibration were obtained by using indium as the standard. Reported values of T_g are those measured as the onset and values of T_m are measured as the endothermic peak maximum.

Small-Angle X-ray Scattering. A 10-m, digital SAXS camera at the National Institute of Standards and Technology (NIST) in Gaithersburg, MD, was used to obtain the scattering data. This camera uses pinhole optics for the collimation of the incident beam and is similar in design to one located at the Oak Ridge National Laboratory.[18] The source was a 12-kW rotating copper anode operated at 45 kV and 180 mA with the Cu $K\alpha$ line selected. The sample to detector distance was set to 2808 mm, and the two-dimensional position sensitive detector was interfaced to a PDP-11 and VAX for graphics and data processing.

Small lead masks with 2-mm diameter holes were used to select homogeneous regions of the sample disks. The sample exposures were between 2 and 4 h with additional exposures for empty beam, dark current, and reference standard. No drift was observed in the empty beam exposures, and the dark current images were similar to others taken before and after these experiments.

Data Treatment. All of the empty beam images were averaged to obtain a data set for correcting the scattering patterns from the samples. When multiple exposures were taken from a sample, the data were also averaged. The contributions from the dark current and from the empty beam (multiplied by the transmission coefficient of each sample, I/I_0) were subtracted from each data set. The data were further corrected to eliminate artifacts from the shadows of the exit window support web, the beam stop, and the edges of the detector. Because these samples exhibited negligible preferred orientation, the data were circularly averaged to increase the intensity and signal-to-noise ratio and to obtain tables of the scattering intensity, I, as a function of s, where s is defined as $s = 2(\sin\theta)/\lambda$. ($\theta$ is half the full scattering angle.)

Thermal Background Correction. To make use of the scattering data at relatively large scattering angles, a correction must be made for the large thermal background scattering. The importance of this correction and several methods for making it have been described by Tyagi and McGrath.[19] We selected the method of generating a Guinier plot, ln (I) vs s^2, and doing a visual linear estimation to the data at large s values, where the scattering from the lamella approaches zero and only the thermal background contribution remains. This linear estimation at large s values is extrapolated to $s = 0$ to obtain an equation for the angularly dependent thermal background correction which is then subtracted from the measured intensity.

Data Presentation. To obtain information on the crystalline lamellae size and spacing and on the interface between crystalline and amorphous regions, the scattering intensities, I, were plotted as a function of s in three ways: Is^2 vs s, referred to as a Lorentz-corrected plot; ln (Is^4) vs s^2, referred to as a modified Porod plot; and in the Fourier inverted form, discussed below.

Fourier-Inverted SAXS Data. Additional morphological information is available from a system that contains a lamellar type structure via the one-dimensional correlation function, $\gamma_{(x)}$. The fully background corrected scattering intensity is related to $\gamma_{(x)}$ as shown in eq 1. Note that this function contains the

$$\gamma_{(x)} = \int_0^\infty I_{(s)} s^2 \cos(2\pi x s)\, ds \qquad (1)$$

Lorentz correction. The correlation function in its most simple sense is the Fourier inversion of the Lorentz-corrected scattering intensity as a function of s. The function represents the probability of finding physical mass or electron density as a function of distance, x, within the material from an origin or zero position which, in our case, can be taken as being the center of a single crystalline lamella. An interactive Fortran computer program was written to execute (on a DEC VAX computer) the Fourier inversion indicated in the above equation. Valuable information can be extracted from the Fourier inverted data, including the interlamellar spacing or long period, denoted L, the lamella thickness, denoted C, the overall (bulk) volume fraction crystallinity, denoted V_c, and the local linear crystallinity, denoted V_c'.[14-17] An example of a computed correlation function is shown in Figure 1 for a 75/25 nylon 66/nylon 3Me6T blend annealed at 155 °C, indicating these quantities and their estimation.

Results and Discussion

Thermal Analysis of the Blends. The general thermal properties measured, T_g, T_m, and heat of fusion, were found to be in approximate agreement with previous work.[6] As mentioned in our introductory comments, it has also been shown that amorphous blends of nylon 6 and nylon 66, respectively, containing nylon 3Me6T exhibit singular and abrupt T_g behavior consistent with miscibility. However, after crystallization of the aliphatic polyamide component, blends in the middle range of composition exhibit broad and inhomogeneous T_g characteristics. This behavior is very reproducible and is observed in blends of either nylon 6 or nylon 66 with nylon 3Me6T. Examples illustrating this are provided in Figure 2, showing the results of thermal analysis of the samples blended for these SAXS studies. It is worth noting the contrast between thermogram C, a blend containing only 25% by weight of the nylon 3Me6T, and the remaining thermograms. The former blend exhibits a heat-capacity change at T_g, ΔC_p, which is typical for a semicrystalline polyamide, and it occurs over a relatively narrow temperature range. The remaining thermograms all show a broad and inhomogeneous T_g behavior. Since annealing took place for an extended period of time above the T_g of both polymers in the blends, we can assume that the volume fractions of amorphous and crystalline material had reached

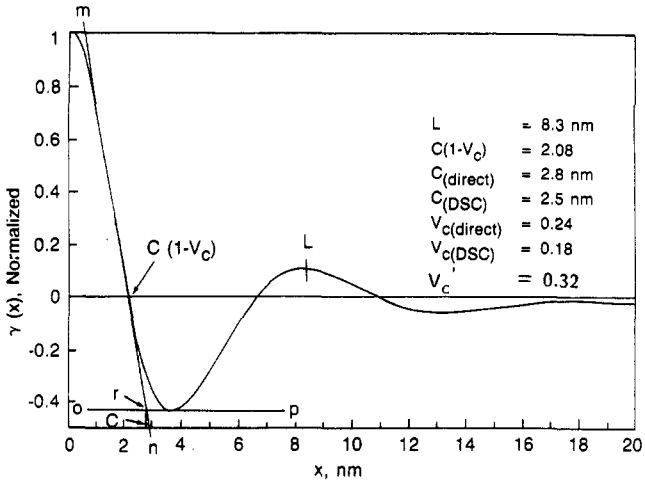

Figure 1. Correlation function plot for the 75:25 nylon 66/nylon 3Me6T blend showing how information can be extracted from this data: *mn* is an extrapolation of the linear portion of the $\gamma_{(x)}$ function. *mn* crosses the $\gamma_{(x)} = 0$ axis at a point giving the value of the expression $C(1 - V_c)$, where V_c is the overall (bulk) volume fraction crystallinity and C is the average lamella thickness. The extrapolation of *mn* to $x = 0$ gives the value of the invariant, Q, for unnormalized data. *op* is drawn tangent to the minimum of the $\gamma_{(x)}$ function and intersects *mn* at point *r*. The x value of point *r* gives C. L, the average value for the long period, is given by the first maximum of the $\gamma_{(x)}$ function. The "local or linear crystallinity", V_c', is given by C/L, which can be very different from V_c, if the system is not homogeneous. Tabulated values for $C(1 - V_c)$, C, L, V_c, and V_c', are indicated on the figure. Quantities referred to as "direct" are obtained directly from the correlation function. Quantities referred to as "(DSC)" are obtained by using the DSC determined value for V_c in the expression $C(1 - V_c)$. (After Strobl and Schneider, ref 17).

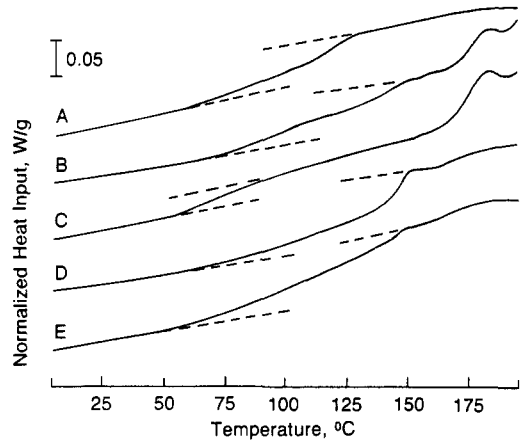

Figure 2. Thermograms of nylon blends used in small-angle X-ray studies: A, nylon 6/nylon 3Me6T (50%), 200 °C/16 h; B, nylon 6/nylon 3Me6T (50%), 155 °C/16 h; C, nylon 6/nylon 3Me6T (25%), 155 °C/16 h; D, nylon 66/nylon 3Me6T (75%), 155 °C/16 h; E, nylon 66/nylon 3Me6T (50%), 155 °C/16 h.

a steady state. Moreover, because of these conditions and the fact that the thermograms were obtained immediately after annealing the samples, we can also assume that the region of interest in the thermograms, 0–150 °C, is not adulterated by any aging or multiple melting phenomena. Finally, despite the rather wide transition range, in some cases up to 100 °C, it can also be seen that values of ΔC_p ($\simeq$0.36→0.4 J/gK) associated with T_g are of a magnitude expected (cf. nylon 3Me6T, $\Delta C_p = 0.39$ J/gK,[6] and noncrystalline nylon 6, $\Delta C_p = 0.847$ J/gK).[20] Thus, the broad and inhomogeneous T_g behavior of the annealed blends other than C is clearly real and is not the result of various artifacts; however, its origins and disposition to investigation by SAXS are not certain. We will explore these possibilities in the following sections.

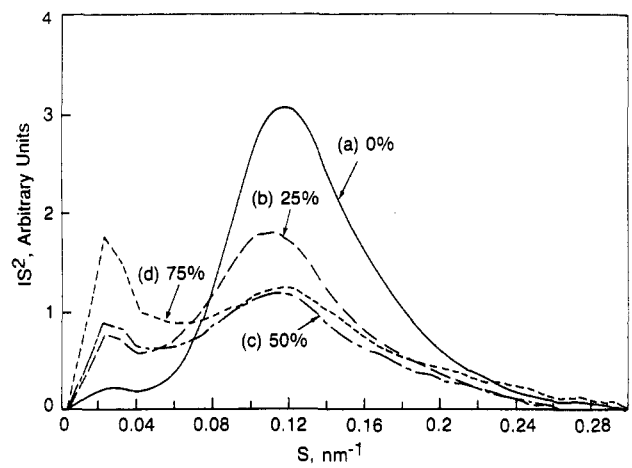

Figure 3. Lorentz-corrected data plot for nylon 6/nylon 3Me6T blends annealed at 155 °C for 16 h: (a) 0% nylon 3Me6T; (b) 25% nylon 3Me6T; (c) 50% nylon 3Me6T; (d) 75% nylon 3Me6T.

Scattering of Nylon 6. Unoriented nylon 6 has a micromorphology which is similar, in many respects, to other semicrystalline polymers when it is observed by transmission electron microscopy (TEM).[21] The largest structural units, spherulites, consist of individual crystalline sheets (lamellae) which alternate with noncrystalline regions to form stacks or domains which radiate outward from the spherulite center. Within a domain the lamella faces are parallel and they tend to have a characteristic thickness and separation distance. However, the orientations of the lamellae in neighboring domains are uncorrelated. Noncrystalline nylon 6 may exist between the lamellae (interlamellar regions), between the domains (interfibrillar regions), or between the spherulites (interspherulitic regions).

This morphology is less ordered compared to other semicrystalline polymers such as polyethylene or poly(ethylene oxide)[14]—the nylon 6 lamellae stacks are short, containing only ~2.5 lamella, and the lateral dimensions of the stacks are small, ~8 nm.[21,22] Consequently, the SAXS peaks are broader.

Scattering of the Blends. The densities of nylon 3Me6T and noncrystalline nylon 6 are ~1.12 and 1.08 g/cm^3, respectively (Table I), and this results in their having nearly equal electron densities. The density of crystalline nylon 6 is 1.24 g/cm^3 (Table I). This means that the crystalline nylon 6 will produce discernible scattering in a matrix consisting of a mixture of noncrystalline nylon 6 and nylon 3Me6T. Noncrystalline nylon 6 in a matrix of nylon 3Me6T or nylon 3Me6T in a matrix of noncrystalline nylon 6 would produce only very weak scattering which would be masked by the much more intense scattering from the nylon 6 crystalline lamellae. These features of the blend system allow the nylon 6 crystalline lamella to be easily observed, however, other micromorphological features could be lost because of the lack of scattering contrast between noncrystalline nylon 6 and nylon 3Me6T. This discussion is expected to also apply to nylon 66 because of the similarities of its amorphous and crystalline densities to those of nylon 6 (see Table I).

The Interlamellar Spacing *L*. The Long Period. Plots of the SAXS data in the Lorentz corrected form, Is^2 vs s, for all the blends investigated are shown in Figures 3, 4, and 5. There is a substantial decrease in scattering intensity as the nylon 6 is diluted with the nylon 3Me6T. By substituting the s value at the maximum of each plot in Bragg's law, an average value for the inter-

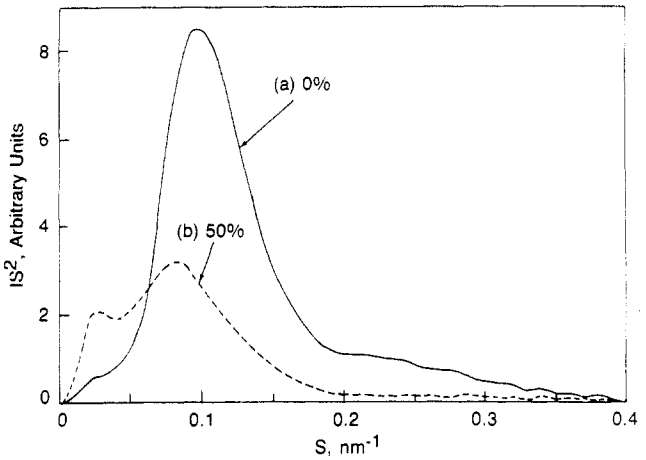

Figure 4. Lorentz-corrected data plot for nylon 6/nylon 3Me6T blends annealed at 200 °C for 16 h: (a) 0% nylon 3Me6T; (b) 50% nylon 3Me6T.

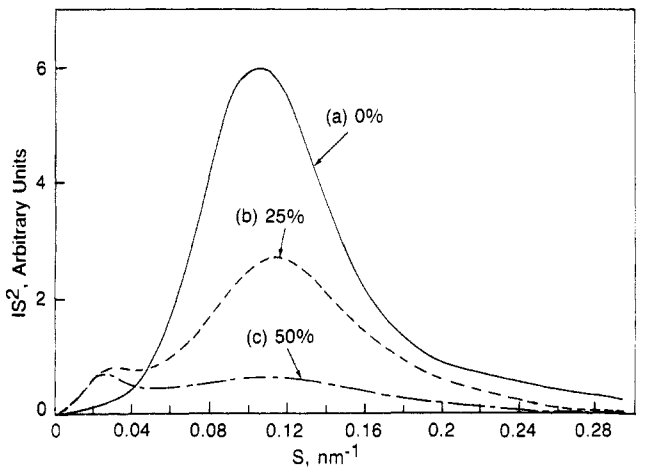

Figure 5. Lorentz-corrected data plot for nylon 66/nylon 3Me6T blends annealed at 155 °C for 16 h: (a) 0% nylon 3Me6T; (b) 25% nylon 3Me6T; (c) 50% nylon 3Me6T.

lamellar spacing or long period, L, can be obtained (Table II, column a). It is observed that the L values are relatively constant in relation to blend composition. The L value for the 75/25 nylon 6/nylon 3Me6T sample (which has a "normal" DSC thermogram) shows a marginal increase and the L value for the 50/50 nylon 6/nylon 3Me6T sample annealed at 200 °C shows a definite increase. The initial hump in these Lorentz-corrected scattering curves at low values of s, especially obvious for the blends with high nylon 3Me6T content, can be considered to arise from increasing long-range heterogeneity of the blend systems as the nylon 6 spherulites are diluted with nylon 3Me6T. Specifically, this scattering may arise from isolated spherulites—the "heterogeneity scattering", I_{sa}, defined by Strobl and Schneider[17]—however, our systems are "volume filled" with spherulites at all blend ratios, which should move such scattering to unobservably small angles. We consider isolated domains (stacks of lamella) or individual isolated lamella to be other possible sources of this scattering. This very low-angle scattering is monotonic and does not have the apperance of a "peak" until it is Lorentz corrected; thus, it is not a Bragg reflection.

It is of interest to note that the values of L obtained by this method for pure nylon 6 annealed at the two different temperatures are essentially identical with those reported previously.[22] The curves produced by Fourier inversion of the Lorentz-corrected scattering data for both types of blends are shown in Figures 6, 7, and 8. From these figures, the L values are simply the x axis value at the position of the first maximum (Table II, column b). Again, it is observed (with the exceptions mentioned above) that L is relatively constant in relation to blend composition and that the values obtained from both methods agree. As may be expected, the 200 °C annealing temperature produces a slightly larger value of L, and, for the 50/50 blend annealed at this temperature, the L value increases 23% over the L value obtained for nylon 6. Figure 9 includes a plot of the L spacings obtained for the nylon 6/nylon 3Me6T system annealed at 155 °C.

The type of plot used to present X-ray scattering or diffraction data warrants further comment because the choice of plot can affect the L spacings obtained. In the general case where the SAXS data from semicrystalline polymers is being examined, L values obtained from the Lorentz-corrected plots are preferred; however, in the case of nylon 6, the Lorentz corrected values may not be the most appropriate because of the poorly defined lamellar structure of nylon 6.[22] Matyi and Crist[22] performed an extensive study of the SAXS of nylon 6 and discussed in detail the accuracy of L values obtained by using different plotting methods. We consider the Fourier inverted data obtained from the Lorentz-corrected data to provide the most precise values for L because of the improved peak resolution.

The invariance of L as a function of blend composition is a striking feature of these blends. At an annealing temperature of 200 °C, a definite increase of L for the 50/50 nylon 6/nylon 3Me6T blend is observed. However, this increase is small when compared to other systems where L often increases by a factor of 2 or more, depending upon composition.[11,16] For example, Russell, Ito, and Wignall[16] found the L value for poly(ethylene oxide) (PEO) diluted with atactic poly(methyl methacrylate) (PMMA) to increase from a value of 23 nm for neat PEO to 40 nm for a 70/30 PEO/PMMA blend (an increase of 74%) and to increase all the way to 94.5 nm for a 50/50 blend (an increase of 311% (!)). Khambatta, Warner, Russell, and Stein[11] found the L value for poly(caprolactone) diluted with poly(vinyl chloride) to increase from 16.1 to 32.2 nm for a 50/50 blend, an increase of 100%. These results can be compared to the measured increase in L of 23% for a 50/50 blend of our nylon 6/nylon 3Me6T system annealed at 200 °C. The only other known instances where this invariant L behavior has been noted is in blends of atactic/isotactic polystyrene[12] and in blends of isotactic poly(methylmethacrylate)/poly(ethylene oxide).[14] In the latter blend, there was a strong indication that the blend was not completely miscible, a feature that could also explain the observed insensitivity of L to blend composition.

For compatible mixtures, the observation of a large increase in the value of L with increasing content of the noncrystallizable component implies that the latter is incorporated within the interlamellar regions.[11,14-16] An observed independence of L with increasing content of the noncrystallizable component implies that the latter is being rejected from the interlamellar regions as the crystallizable component crystallizes.[12] This second case describes our experimental results for the nylon 6/nylon 3Me6T system—it is like a type of crystallization-induced phase separation—and we thus interpret it to mean that the nylon 3Me6T resides mainly in the interfibrillar and interspherulitic regions of the crystallized blends. The 75/25 nylon 6/nylon 3Me6T sample and the 50/50 nylon 6/nylon 3Me6T sample annealed at 200

Table II
SAXS Derived Data for the Blends

sample		interlamellar spacing L, nm (a)	interlamellar spacing L, nm (b)	diffuse boundary thickness D, nm (c)	lamella thickness C, nm (d)	lamella thickness C, nm (e)	amorphous layer thickness A, nm (f)	volume fraction crystallinity V_c (bulk) (g)	volume fraction crystallinity V_c (bulk) (h)	V_c' (local) (i)
Nylon 6/Nylon 3Me6T Samples Annealed at 155 °C for 16 h										
n6-n3Me6T	0%	8.5	8.0	0.72	2.8	2.7	5.3	0.31	0.29	0.34
n6-n3Me6T	25%	9.2	8.6	0.65	2.9	2.9	5.7	0.24	0.23	0.34
n6-n3Me6T	50%	9.0	8.7	0.55	2.9	2.7	6.0	0.18	0.15	0.32
n6-n3Me6T	75%	8.3	7.8	0.36	2.6	2.5	5.3	0.10	0.06	0.33
Nylon 6/Nylon 3Me6T Samples Annealed at 200 °C for 16 h										
n6-n3Me6T	0%	10.3	9.3	0.78	2.9	3.2	6.1	0.28	0.35	0.33
n6-n3Me6T	50%	11.9	11.4	0.82	3.7	3.5	7.9	0.22	0.17	0.32
Nylon 66/Nylon 3Me6T Samples Annealed at 155 °C for 16 h										
n66-n3Me6T	0%	9.7	9.0	0.55	2.8	2.7	6.3	0.28	0.27	0.31
n66-n3Me6T	25%	8.8	8.3	0.55	2.8	2.5	5.8	0.24	0.18	0.32
n66-n3Me6T	50%	9.1	8.6	0.00	2.6	2.6	6.0	0.13	0.12	0.30

[a] Obtained from Is^2 vs s plot ("Lorentz corrected"). [b] Obtained from Fourier-inverted data. [c] Obtained from ln (Is^4) vs s^2 plot ("modified Porod"). [d] Obtained from Fourier-inverted data. [e] Obtained from Fourier-inverted data modified by DSC data. [f] Obtained by the difference $A = L - C$. [g] Obtained from Fourier-inverted data. [h] DSC values: using ΔH_f values of 230 J/g for nylon 6 and 300 J/g for nylon 66 (Wunderlich, B. *Macromolecular Physics*; Academic Press: New York, London, Toronto, Sydney, San Francisco, 1980; Vol. 3, pp 56–7) and corrected for the densities of the amorphous and crystalline phases (Table I). [i] Obtained from the ratio $V_c' = C/L$. Obtained from Fourier-inverted data.

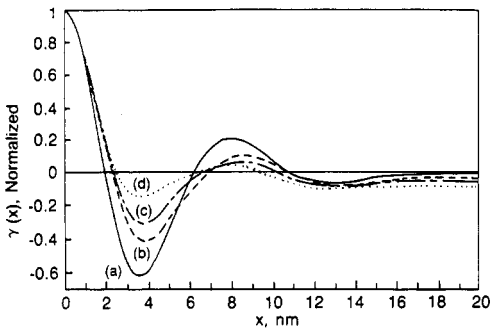

Figure 6. Correlation function plot for nylon 6/nylon 3Me6T blends annealed at 155 °C for 16 h: (a) 0% nylon 3Me6T; (b) 25% nylon 3Me6T; (c) 50% nylon 3Me6T; (d) 75% nylon 3Me6T.

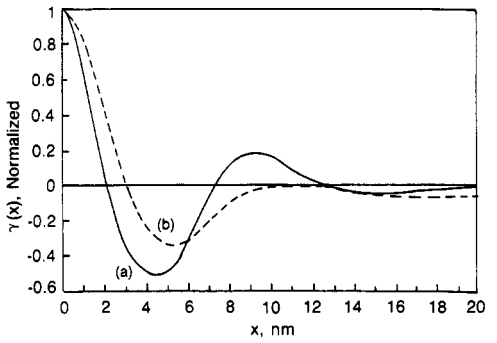

Figure 7. Correlation function plot for nylon 6/nylon 3Me6T blends annealed at 200 °C for 16 h: (a) 0% nylon 3Me6T; (b) 50% nylon 3Me6T.

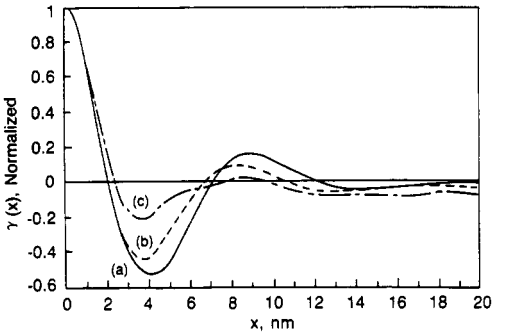

Figure 8. Correlation function plot for nylon 66/nylon 3Me6T blends annealed at 155 °C for 16 h: (a) 0% nylon 3Me6T; (b) 25% nylon 3Me6T; (c) 50% nylon 3Me6T.

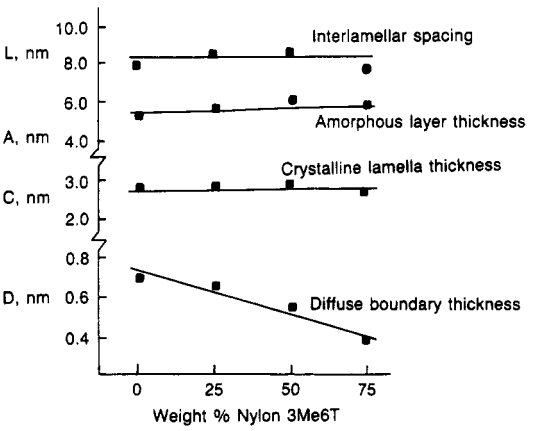

Figure 9. Effect of nylon 3Me6T content on the nylon 6 crystalline micromorphology for nylon 6/nylon 3Me6T blends.

°C appear to be exceptions to this generalization; in fact, their L value changes can be explained by assuming the opposite behavior—interlamellar incorporation of the nylon 3Me6T—so that the generalization we have made is open to question; however, the behavior of these two samples will be analyzed in more detail in the following section. The presence of nylon 3Me6T in the interfibrillar regions has little effect on the fine texture structure and periodicity measured by SAXS. If nylon 3Me6T is excluded from the interlamellar regions, then these regions must of necessity be highly enriched in nylon 6, leading to a heterogeneous amorphous phase. This observation in itself may explain the usual glass transition behavior of some of the blends; however, other reasonable morphological situations could also be advanced to account for this.

Lamellae Thickness (C), Overall (Bulk) Crystallinity (V_c), and Local Linear Crystallinity ($V_c' = C/L$). We used the correlation function derived from the experimental data (Figures 6 through 8) to deduce average values for the thicknesses of the crystalline lamellae, C, the overall (bulk) crystallinity, V_c, and the local linear crystallinity, $V_c' = C/L$. Several methods are available for obtaining numerical values for these quantities.[14,16,17] C can be obtained in a graphical manner, as shown in Figure 1, from the intersections of the lines mn and op. We refer to this as the "direct" determination of C. Values

for C, so determined appear in column d of Table II. These values are rather constant for all the blends which were annealed at 155 °C; Figure 9 includes a plot of C as a function of blend composition for the nylon 6/nylon 3Me6T system. To determine V_c, one takes the value of x at $\gamma_{(x)} = 0$, which gives the numerical value of the quantity $C(1 - V_c)$, and substitutes the graphical value of C into it, yielding a value for V_c which we call "direct". Values for V_c, so determined, appear in column g of Table II. One can take the DSC determined value for V_c (these values appear in column h of Table II), substitute it into the quantity $C(1 - V_c)$, and determine a "DSC-modified" value for C. These values appear in column e of Table II. The agreement between the two methods for obtaining C ("direct" and "DSC modified") and the two methods for obtaining V_c ("direct" and DSC) is good. It is interesting to note that the values for V_c obtained by both methods can be obtained, approximately, by simply multiplying the SAXS or DSC determined value for the 100% nylon 6 (or 66) sample by the volume fraction of that component in the blend. This means that the nylon 6 (or 66) in the blends tends to obtain its maximum degree of crystallinity even in the presence of increasing amounts of nylon 3Me6T.

An important concept in the above analysis is that the quantity V_c is an overall (bulk) crystallinity, which can be distinguished from a local linear crystallinity, V_c', given by $V_c' = C/L$. This is the "inhomogeneous systems case" described by Strobl and Schneider,[17] and their model is versatile enough to handle this situation, provided the entire SAXS curve is Fourier transformed (which we have done). Values for V_c' are given in column i of Table II and are very constant, a necessary consequence of the invariance of L and C. *The observation of constant V_c' values with concurrently decreasing V_c values as the concentration of nylon 3Me6T increases can be reconciled only by assuming rejection of the nylon 3Me6T from the interlamellar regions.* The relative behaviors of V_c and V_c' thus provide a proof of such behavior in addition to that provided by the constancy of L. Further, the 0.32 value of V_c' for the 50/50 nylon 6/nylon 3Me6T blend annealed at 200 °C and the 0.34 value of V_c' for the 75/25 nylon 6/nylon 3Me6T blend annealed at 155 °C suggest that the increases in L observed for these two systems represent minimal interlamellar incorporation of the nylon 3Me6T: The increases in L are accompanied by measured increases in C, and the ratio C/L remains essentially constant.

Diffuse Boundary Thickness (D) and the Amorphous Layer Thickness (A). Two lamellae of thickness C′ are separated (center-to-center) by the long spacing, L, and are connected by diffuse boundary layers, D, to the interlamellar amorphous region, A'. The diffuse boundary layer, D, can be considered a separate entity; however, the geometry of the correlation function analysis is such that the thicknesses obtained, C and A, implicitly include the thickness of D. We denote such quantities (containing D) with the lack of a prime (′). The following relationships hold:

$$A = L - C \tag{2}$$

$$A' = A - D \tag{3}$$

$$C' = C - D \tag{4}$$

The values for A were determined from eq 2; they appear in column f of Table II and also in a plot on Figure 9 for the nylon 6/nylon 3Me6T system. The relative constancy of the amorphous layer thickness, A, is a result of the invariance of C and L combined with the feature

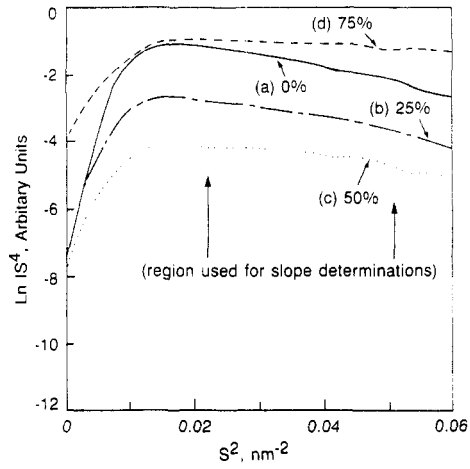

Figure 10. Modified Porod data plot for nylon 6/nylon 3Me6T blends annealed at 155 °C for 16 h: (a) 0% nylon 3Me6T; (b) 25% nylon 3Me6T; (c) 50% nylon 3Me6T; (d) 75% nylon 3Me6T.

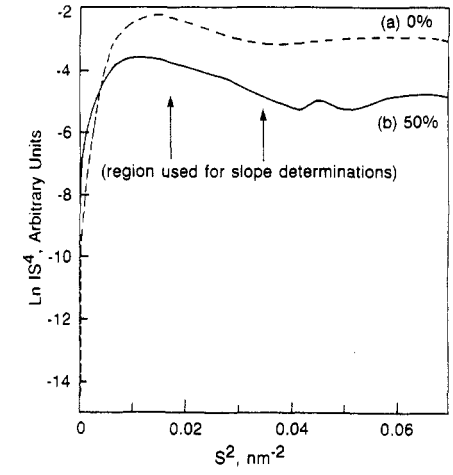

Figure 11. Modified Porod data plot for nylon 6/nylon 3Me6T blends annealed at 200 °C for 16 h: (a) 0% nylon 3Me6T; (b) 50% nylon 3Me6T.

that the values for D are relatively small, as will be discussed immediately below. This constancy of A is further evidence that there is minimal incorporation of nylon 3Me6T into the interlamellar regions. (The 50/50 nylon 6/nylon 3Me6T blend annealed at 200 °C is an exception in that its A value increases significantly; however, C also increases, as was discussed above.)

The values for the thickness of the diffuse boundary, D, were not obtained from the correlation function; instead, we used modified Porod plots, ln (Is^4) vs s^2, which are shown in Figures 10, 11, and 12. The negative slopes of these plots at s values greater than their maxima indicate the existence of a diffuse interface between the crystalline lamellae and the noncrystalline interlamellar regions and allow a numerical value for its thickness to be estimated.[19] From a straight line fit to the linear region of each plot (these regions are indicated on the figures) values of the slopes are obtained from which the thickness of the diffuse boundary, D, can be calculated[19] by using eq 5. This model assumes that the electron density gradient across the diffuse boundary is sigmoidal. Values obtained for the diffuse boundary thicknesses are given in column c of Table II and are shown in Figure 9 for the nylon 6/nylon 3Me6T system.

$$D^2 = -\text{slope}/8\pi^2 \tag{5}$$

A decline in diffuse boundary thickness is observed as the nylon 3Me6T concentration increases. We can spec-

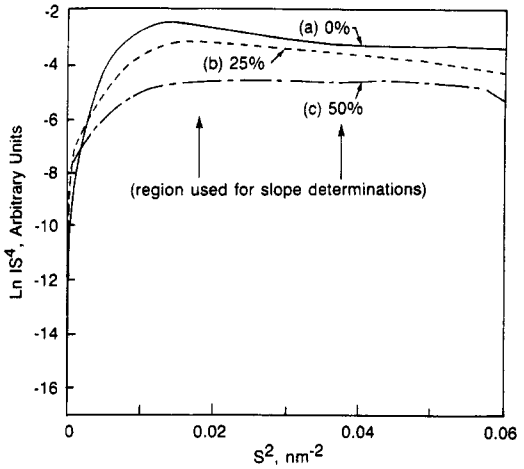

Figure 12. Modified Porod data plot for the nylon 66/nylon 3Me6T blends annealed at 155 °C for 16 h: (a) 0% nylon 3Me6T; (b) 25% nylon 3Me6T; (c) 50% nylon 3Me6T.

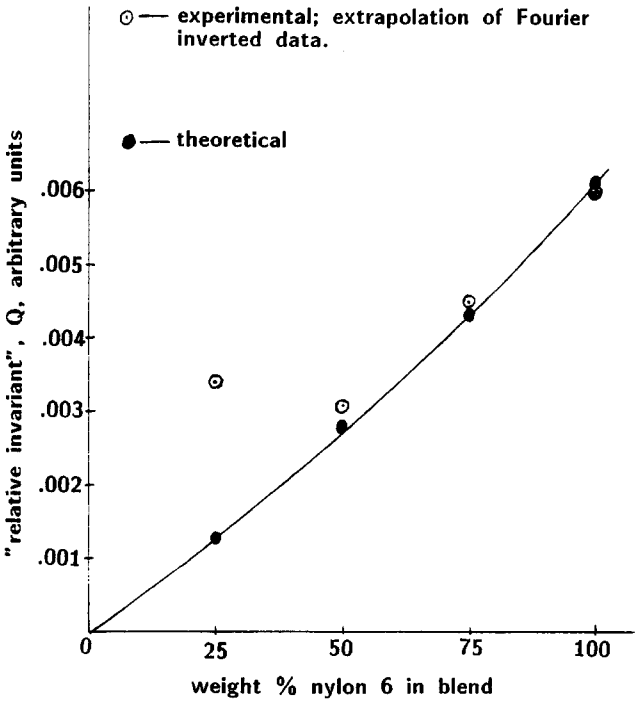

Figure 13. Theoretical and experimental invariants for the nylon 6/nylon 3Me6T blends annealed at 155 °C for 16 h.

ulate that the slower rate of crystallization, concurrent with increasing nylon 3Me6T content, leads to a more ordered crystalline structure which, in turn, is consistent with smaller dimensions of the crystal/amorphous interfacial thickness—after a nylon 6 crystalline lamella forms and reaches its maximum dimensions, the nylon 6 chains have sufficient time such that they can assume their amorphous orientations in a short distance.

Blends of nylon 66 and nylon 3Me6T exhibit behavior analogous to that observed for the nylon 6/nylon 3Me6T system. The values of L and A show no tendency to increase with increasing nylon 3Me6T content, and the values of C and D remain constant. We therefore conclude that for the nylon 66/nylon 3Me6T system, as with the nylon 6/nylon 3Me6T system, the nylon 3Me6T is rejected or excluded from the nylon 66 interlamellar regions as the nylon 66 crystallizes. Annealing temperature appears to be a more important variable than the type of crystalline nylon because the values for L and C were observed to increase with increasing nylon 3Me6T content for the nylon 6/nylon 3Me6T system annealed at 200 °C.

Evaluation of the "Relative Invariant". The experimentally measured transmission coefficient for each sample, I/I_0, was used to normalize the relative scattering intensities measured for each sample to what would be obtained for samples of constant thickness. This was done by dividing the scattering intensities for each data set by the expression $(I/I_0)(\ln (I_0/I))$. The unnormalized Fourier transformed SAXS data curves (not shown) were then used to obtain the "relative invariants" by extrapolation of the straight portion of the Fourier inverted curves, line mn in Figure 1, to $x = 0$. The results obtained are shown on Figure 13.

A crude physical model for our system is that it is a two-phase mixture consisting of nylon 6 crystallites in an amorphous matrix. Values for the theoretical invariant, Q, from such a mixture were calculated and are shown on Figure 13. The Q values are observed to roughly follow the nylon 6 concentration, as expected. It is not known why the experimental value for the 25/75 nylon 6/nylon 3Me6T sample lies so far off the curve. We are currently evaluating the theoretical scattering from a proper model, which consists of three phases: nylon crystalline lamella, an interlamellar amorphous phase, and an "extralamellar" amorphous phase.

Conclusions

The crystallization of nylon 6 and nylon 66, each, in blends containing a noncrystallizable polymer diluent, results in the rejection of the latter component from the interlamellar regions. At the lower diluent levels this interpretation is less certain; however, specific blends initially thought to be exceptions to this generalization because of observed increases in their long periods, probably have minimal amounts of interlamellar incorporation because their local linear crystallinities remain constant. While this segregation behavior is not unique, it is still a rather rare phenomena and can be related to the diffusion of species away from developing crystal surfaces. We have not considered any potential contribution from the crystal forming habits of aliphatic polyamides. The development of heterogeneous mixed amorphous regions, resulting form the crystallization process, provides a rational explanation for unusual thermal behavior in the blends observed by calorimetry. The results of the scattering therefore support the initial suggestion that the apparent phase inconsistency was morphological in origin rather than the result of immiscibility of the components of the blends.

Acknowledgment. We thank Dr. R. M. Briber of NIST for performing initial exploratory studies on these materials and for helping make the SAXS facility available to us. We thank Dr. John Owens of the General Motors Research Laboratories for his instructive comments.

References and Notes

(1) Keith, H. D.; Padden, F. J. *J. Appl. Phys.* **1964**, *35*, 1270.
(2) Keith, H. D.; Padden, F. J. *J. Polym. Sci., Part B* **1987**, *25*, 2371; **1988**, *26*, 703.
(3) Briber, R. M.; Khoury, F. *Polymer* **1987**, *28*, 38.
(4) Keith, H. D.; Padden, F. J. *Polymer* **1986**, *27*, 1463.
(5) Keith, H. D.; Padden, F. J.; Russell, T. P. *Macromolecules* **1989**, *22*, 666.
(6) Ellis, T. S. *Polymer* **1988**, *29*, 2015.
(7) Ellis, T. S. *Macromolecules* **1989**, *22*, 742.
(8) Ellis, T. S. *Polymer*, in press.
(9) Li, X.; Hsu, S. L. *J. Polym. Sci., Polym. Phys. Ed.* **1984**, *22*, 1331.
(10) Tekely, P.; Laupretre, F.; Monnerie, L. *Polymer* **1985**, *26*, 1081.

(11) Khambatta, F. B.; Warner, F. P.; Russell, T. P.; Stein, R. S. *J. Polym. Sci., Part B* **1976**, *14*, 1391.
(12) Warner, F. P.; MacKnight, W. J.; Stein, R. S. *J. Polym. Sci., Polym. Phys. Ed.* **1977**, *15*, 2113.
(13) Russell, T. P.; Stein, R. S. *J. Polym. Sci., Polym. Phys. Ed.* **1983**, *21*, 999.
(14) Silvestre, C.; Cimmino, S.; Martuscelli, E.; Karasz, F. E.; MacKnight, W. J. *Polymer* **1987**, *28*, 1190.
(15) Hahn, B. R.; Herrman-Schnherr, O.; Wendorff, J. H. *Polymer* **1987**, *28*, 201.
(16) Russell, T. P.; Ito, H.; Wignall, G. D. *Macromolecules* **1988**, *21*, 1703.
(17) Strobl, G. R.; Schneider, M. *J. Polym. Sci., Polym. Phys. Ed.* **1980**, *18*, 1343.
(18) Hendricks, R. W. *J. Appl. Crystallogr.* **1978**, *11*, 15.
(19) Tyagi, J.; McGrath, J. E.; Wilkes, G. L. *Polym. Eng. Sci.* **1986**, *26*, 1371.
(20) Gaur, U.; Lau, S.; Wunderlich, B. *J. Phys. Chem. Ref. Data* **1983**, *12*, 88.
(21) Galeski, A.; Argon, A. S.; Cohen, R. E., *Makromol. Chem.* **1987**, *188*, 1195.
(22) Matyi, R. J.; Crist, B., Jr. *J. Polym. Sci., Polym. Phys. Ed.* **1978**, *16*, 1329.

Registry No. Trogamid T, 9071-17-4; Nylon 6, 25038-54-4; Nylon 66, 32131-17-2.

Nuclear Magnetic Resonance Relaxation Studies of Plant Polyester Dynamics. 1. Cutin from Limes

Joel R. Garbow and Ruth E. Stark*

Chesterfield Village NMR Center, Monsanto Company, St. Louis, Missouri 63198, and Department of Chemistry, College of Staten Island, City University of New York, Staten Island, New York 10301

Received September 18, 1989

ABSTRACT: Magic angle spinning (MAS) ^{13}C NMR results are reported for intact lime cuticle and its two major components, cutin and wax. DPMAS and CPMAS experiments permit determination of the numbers of relatively mobile and immobile carbons in each biopolymer sample. $T_{1\rho}(C)$ and $T_1(C)$ relaxation experiments characterize kilohertz- and megahertz-regime motions, respectively; they indicate that motional restrictions are present at cross-links of the cutin polymer and along alkyl chains of the wax alone. Values of $\langle T_{1\rho}(C)\rangle$ and $\langle T_1(C)\rangle$, which differ significantly for analogous carbon sites of cutin and wax individually, approach common values for the two materials in the intact lime cuticle. These results, together with measurements of $T_{1\rho}(H)$, provide evidence for hydrophobic association within the plant cuticle of the long aliphatic chains of cutin and wax.

Introduction

It is well established that molecular motion provides a link between polymer molecular structure and bulk mechanical behavior.[1] Particular attention has been focused on local segmental reorientation, though overall conformational changes and chain translation also help to determine properties such as the modulus of a polymeric material. Magnetic resonance experiments have proven to be a rich source of such dynamic information about polymers.[2,3]

Much of the work in this area has focused on synthetic compounds. For example, efforts to understand the piezoelectric and mechanical properties of poly(vinylidene fluoride) have included ^1H and ^{19}F NMR relaxation studies of chain dynamics for both the crystalline and amorphous components of this material.[4] The mechanical impact strength of commercial polycarbonates and other glassy polymers has been rationalized in terms of mid-kilohertz main-chain motions, which can be studied via rotating-frame carbon relaxation ($T_{1\rho}(C)$) measurements conducted under cross-polarization magic angle spinning (CPMAS) conditions.[5] The thermoplastic behavior of Hytrel copolyesters has been examined by employing a battery of ^{13}C and ^2H solid-state NMR techniques to characterize the dynamics of individual backbone sites in both hard and soft polymer segments.[3]

The dynamics of natural polymers are no doubt important in understanding their properties as well, though the complexity of such materials has slowed their characterization. For intact plant materials such as lignin, cutin, and suberin, several recent solid-state ^{13}C NMR studies have identified and quantified the principal chemical moieties;[6-10] for cuticular support polymers such as lime cutin, segmental flexibility has been assessed from ^{13}C spin–lattice relaxation ($T_1(C)$) measurements.[9] We report herein an extensive dynamics study of lime cuticle along with its cutin and wax constituents, including determinations of $T_1(C)$, $T_{1\rho}(C)$, and $T_{1\rho}(H)$ and the proportions of liquidlike and solidlike carbons for each plant material. These results are interpreted in terms of the resiliency of the cuticle and its function as a barrier to invasion by fungal pathogens.[11,12]

Materials and Methods

Cuticle from Limes. Following published protocols,[13,14] the peels from 20 limes were treated to remove pectin and cellulose. The resulting cuticular material was either kept intact or treated further to separate the cutin and wax components. A typical preparation yielded 800 mg of cutin polymer and 80 mg of waxes. Samples for solid-state NMR (175–300 mg) were ground

* Author to whom correspondence should be addressed at the College of Staten Island, City University of New York.

0024-9297/90/2223-2814$02.50/0